

Substitutional carbon-dioxygen center in irradiated silicon

Kuganathan, N., Chroneos, A., Christopoulos, S., Postidi, M., Angeletos, T., Sarlis, N. V. & Londos, C. A.

Author post-print (accepted) deposited by Coventry University's Repository

Original citation & hyperlink:

Kuganathan, N, Chroneos, A, Christopoulos, S, Postidi, M, Angeletos, T, Sarlis, NV & Londos, CA 2021, 'Substitutional carbon-dioxygen center in irradiated silicon', Materials Science in Semiconductor Processing, vol. 127, 105661, pp. (In-Press).
<https://dx.doi.org/10.1016/j.mssp.2021.105661>

DOI 10.1016/j.mssp.2021.105661

ISSN 1369-8001

Publisher: Elsevier

© 2021, Elsevier. Licensed under the Creative Commons Attribution-NonCommercial-NoDerivatives 4.0 International

<http://creativecommons.org/licenses/by-nc-nd/4.0/>

Copyright © and Moral Rights are retained by the author(s) and/ or other copyright owners. A copy can be downloaded for personal non-commercial research or study, without prior permission or charge. This item cannot be reproduced or quoted extensively from without first obtaining permission in writing from the copyright holder(s). The content must not be changed in any way or sold commercially in any format or medium without the formal permission of the copyright holders.

This document is the author's post-print version, incorporating any revisions agreed during the peer-review process. Some differences between the published version and this version may remain and you are advised to consult the published version if you wish to cite from it.

Materials Science in Semiconductor Processing

Substitutional carbon-dioxygen center in irradiated silicon

--Manuscript Draft--

Manuscript Number:	
Article Type:	Research Paper
Section/Category:	Semiconductors
Keywords:	Silicon; irradiation; IR spectroscopy; DFT calculations
Corresponding Author:	Marianna S Potsidi National and Kapodistrian University of Athens Athens, GREECE
First Author:	Marianna S. Potsidi
Order of Authors:	Marianna S. Potsidi N. Kuganathan A. Chroneos S.-R. G. Christopoulos T. Angeletos C. A. Londos, Professor
Abstract:	<p>Systematic density functional theory (DFT) calculations were used to predict the lowest energy structure of the substitutional carbon- dioxygen (CsO_2i) defect in silicon (Si). Thereafter, the dipole-dipole interaction method was employed to calculate the local vibration modes (LVM) of this lowest energy structure. We found that the CsO_2i defect is characterized by two LVM frequencies at 1051.4 and 1166.3 cm^{-1}. These values are quite close to experimental bands of earlier studies at 1048 and 1094 cm^{-1} (deviation $\sim 6.5\%$) reported in the literature, both attributed to the CsO_2i defect. In this work, Infrared Spectroscopy (IR) measurements were carried out at room temperature (RT), to study defect signals after electron irradiation in Si samples. Next, isochronal anneals were carried out to monitor the thermal evolution of the bands. We mainly focused on a band at 1048 cm^{-1} grown in the spectra upon annealing out of the 830 cm^{-1} band of the vacancy-oxygen center (VO) and the 861 cm^{-1} band of the carbon interstitial-oxygen interstitial (CiO_i) center. The analysis and examination of the results lead us to suggest that the 1048 cm^{-1} band originates from the CsO_2i complex, formed according to the reaction: $\text{VO} + \text{Ci} \text{ O}_\text{i} \rightarrow \text{CsO}_2\text{i}$. The other band at 1094 cm^{-1} is most probably masked by the very strong band of O_i (1107 cm^{-1}, at RT) in Si.</p>

Substitutional carbon-dioxygen center in irradiated silicon

M. S. Potsidi,^{1,a)} N. Kuganathan,^{2,3} A. Chroneos,^{2,3} S.-R. G. Christopoulos,² T. Angeletos¹ and C. A. Londos,^{1,b)}

¹*National and Kapodistrian University of Athens, Department of Physics, Solid State Physics Section, Panepistimiopolis Zografos, Athens 157 84, Greece*

²*Faculty of Engineering, Environment and Computing, Coventry University, Priory Street, Coventry CV1 5FB, UK*

³*Department of Materials, Imperial College London, London SW7 2AZ, UK*

ABSTRACT

Systematic density functional theory (DFT) calculations were used to predict the lowest energy structure of the substitutional carbon-dioxygen (C_sO_{2i}) defect in silicon (Si). Thereafter, the dipole-dipole interaction method was employed to calculate the local vibration modes (LVM) of this lowest energy structure. We found that the C_sO_{2i} defect is characterized by two LVM frequencies at 1051.4 and 1166.3 cm^{-1} . These values are quite close to experimental bands of earlier studies at 1048 and 1094 cm^{-1} (deviation $\sim 6.5\%$) reported in the literature, both attributed to the C_sO_{2i} defect. In this work, Infrared Spectroscopy (IR) measurements were carried out at room temperature (RT), to study defect signals after electron irradiation in Si samples. Next, isochronal anneals were carried out to monitor the thermal evolution of the bands. We mainly focused on a band at 1048 cm^{-1} grown in the spectra upon annealing out of the 830 cm^{-1} band of the vacancy-oxygen center (VO) and the 861 cm^{-1} band of the carbon interstitial-oxygen interstitial (C_iO_i) center. The analysis and examination of the results lead us to suggest that the 1048 cm^{-1} band originates from the C_sO_{2i} complex, formed according to the reaction: $VO + C_iO_i \rightarrow C_sO_{2i}$. The other band at 1094 cm^{-1} is most probably masked by the very strong band of O_i (1107 cm^{-1} , at RT) in Si.

Keywords: Silicon; irradiation; IR spectroscopy; DFT calculations

Corresponding authors: a) M. S. Potsidi (mpotsidi@phys.uoa.gr) b) C. A. Londos (hlontos@phys.uoa.gr)

INTRODUCTION

As Si is a key material in the semiconductor industry (optoelectronics, nanoelectronics, solar cells and sensors) its quality is important for the functionality of devices. This is affected by impurities and defects introduced in the lattice in the course of material growth and/or of material processing.¹⁻⁶ The understanding of the structure, properties and behavior of defects in Si is highly significant both for scientific and technological reasons.^{1,2}

Oxygen and carbon are the most common impurities unintentionally introduced in the Si lattice, during crystal growth and device processing.⁷⁻¹⁰ Although both are electrically inert in the Si lattice (oxygen as an interstitial, (O_i) and carbon as a substitutional, (C_s)) they can affect the electrical properties of Si upon material processing through the formation of various complexes (for example, thermal donors and oxygen precipitates created upon thermal treatments).^{7,8, 11-14} Additionally, the C and O impurities lead to the formation of a number of complexes upon irradiation and/or implantation. Important among them are the VO, C_iO_i and C_iC_s pairs, which are electrical active and introduce levels in the Si lattice.^{7,8} Their presence leads to performance losses and degradation of the devices.¹⁵⁻²³ Furthermore, upon annealing these defects participate in a variety of reaction channels leading to the formation of numerous second generation complexes.

Here we focus on carbon-oxygen defects and in particular on the C_sO_{2i} defect. This complex has been detected in a number of experiments under different conditions of irradiations carried out at various temperatures. Previous studies have detected two IR bands at 1052 and 1099 cm⁻¹ measured at low temperature and were attributed²⁴ to a C-O complex. These bands were later correlated with the C_sO_{2i} complex, and in particular with two oxygen-related LVMs of its structure.²⁵⁻²⁷ C_sO_{2i} is a second order generation defect and one way to form^{28, 29} is by the interaction of the VO and the C_iO_i pairs upon their annealing around 300 °C. The suggested reaction is: VO + C_iO_i → C_sO_{2i}. Notably, although VO and C_iO_i anneal out mainly by dissociation, a small percentage of them could migrate^{7, 30} as entities and upon their encounter produce the C_sO_{2i} complex. In this scheme, vacancies liberated from the dissociation of VO react with C_iO_i to form in the first place C_sO_i pairs, which then capture O_i from the dissociated C_iO_i pair to form finally C_sO_{2i}. The latter center could also be produced³¹ by the reaction C_i + VO₂ → C_sO_{2i} were C_i are produced by the liberation of the C_iO_i and VO₂ are formed as a result of the VO annealing (VO + O_i →

VO₂). The same reaction was suggested^{32, 33} for irradiations at 400-600 °C. The 1052 and 1099 cm⁻¹ bands have also been reported in thermally treated Si material where it was suggested³⁴ that the capture of oxygen dimers O_{2i} by C_s impurities could lead to the formation of the C_sO_{2i} complex (C_s + O_{2i} → C_sO_{2i}). We note that, in RT measurements the two bands of the complex shift to the values³⁵ 1048 and 1094 cm⁻¹.

In the present study we systematically investigate the lowest energy configuration of the C_sO_{2i} defect using DFT calculations. This structure is then used in dipole-dipole interaction methods to calculate the LVM frequencies of the C_sO_{2i} structure. These were compared with IR spectroscopy measurements.

METHODOLOGY

Experimental methodology

We used Czochralski (Cz-Si) prepolished samples with typical dimensions of 15x10x1.8 mm³. The samples, purchased from MEMC, were initially p- type (boron doped) with resistivity ρ~ 10 Ω cm. The initial oxygen and carbon concentrations were [O_i] = 1x10¹⁸ and [C_s] = 1.6x10¹⁷ cm⁻³, respectively. Float-zone (FZ) samples of [O_i] = 1x10¹⁶ cm⁻³ and [C_s] below detection limits were also used for comparison purposes. The Cz-Si samples were irradiated with 2 MeV electrons with a fluence of 1x10¹⁸ cm⁻² at about 80°C, using the Dynamitron accelerator at Takasaki-JAERI (Japan). After irradiation the samples were subjected to isochronal anneals up to ~600°C in open furnaces, in steps of ~10°C and 20 minutes duration. After each annealing step, IR spectra were recorded at RT by means of a Fourier Transform Infrared spectrometer (JASCO-470 plus) with a resolution of 1cm⁻¹. The two phonon absorption was always subtracted from each spectrum by using a reference sample of equal thickness from FZ material.

Theoretical methodology

Spin-polarised DFT calculations as implemented in the VASP code^{36, 37} were used. This code uses plane wave basis sets and projected augmented wave (PAW)³⁸ potentials to solve the standard Kohn-Sham (KS) equations. All calculations were performed using a supercell consisting of 250 Si atoms. The generalized gradient approximation (GGA) as parameterised by Perdew, Burke and Ernzerhof (PBE)³⁹ was used to model the exchange correlation effects. A plane wave basis set with a cut-off of 500 eV and a 2 × 2 × 2 Monkhorst-Pack⁴⁰ k-point mesh which yielded 8 irreducible

k-points were used. Geometry optimisations were performed under constant pressure conditions (both positions of atoms and lattice parameters were relaxed simultaneously) with the aid of a conjugate gradient algorithm.⁴¹ All optimised configurations reached the required accuracy of convergence (force tolerance 0.001 eV/Å and stress tensor 0.002 GPa). Bader charge analysis⁴² as implemented in the VASP code was carried out to determine the charges on the C, Si and O atoms. The dispersion interactions were included in a semi-empirical form as implemented by Grimme *et al.*⁴³ The efficacy of electronic structure simulations to model group IV semiconductors and the importance of related defects has been demonstrated in previous works.⁴⁴⁻⁴⁷

RESULTS AND DISCUSSION

Fig. 1 displays the IR spectra of the Cz-Si samples recorded after irradiation and at a characteristic temperature of 350 °C in the course of 20 min isochronal anneals performed after the irradiation. They represent a segment of the whole spectrum in the range 800-1100 cm⁻¹. In this range we observe LVM bands of well-known defects as VO (830 cm⁻¹), C_iO_i (861 cm⁻¹), C_iO_i(Si_i) (936, 1020 cm⁻¹) after irradiation (lower curve), and VO₂ (888 cm⁻¹) as well as bands at 1020 and 1048 cm⁻¹ at 350 °C (upper curve).

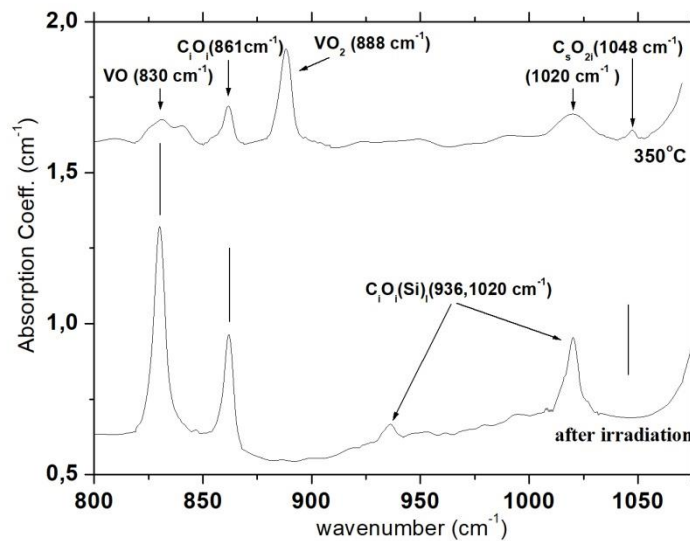


Fig. 1 Characteristic segments of the IR spectra of the Cz-Si samples after irradiation and at 350 °C of the isochronal anneal sequence.

The band at 1020 cm^{-1} in the upper curve is different from that at 1020 cm^{-1} of the lower curve, originated⁴⁸ from the $\text{C}_i\text{O}_i(\text{Si}_i)$ complex and annealed out at $\sim 200\text{ }^\circ\text{C}$. The investigation of the latter band at 1048 cm^{-1} is the main aim of this work.

Fig. 2 demonstrates the evolution with temperature of the VO, C_iO_i , VO_2 and 1048 cm^{-1} bands. 1048 cm^{-1} band seems to arise in the spectra upon annealing out of the VO and the C_iO_i defects. It has been correlated²⁵⁻²⁸ with the C_sO_{2i} complex. In the work below, we have used theoretical results employing DFT and dipole-dipole approximation methods, which we combined with experimental results from IR spectroscopy to investigate the above attribution.

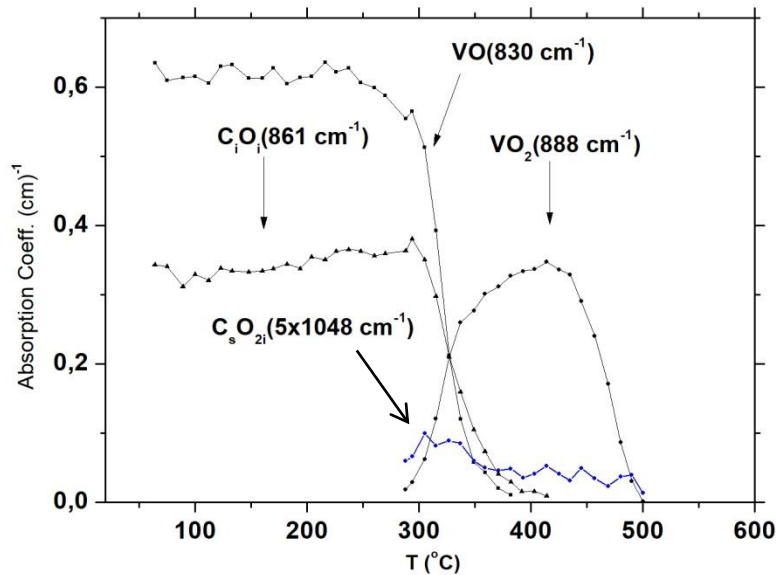


Fig. 2 Thermal evolution of the VO, C_iO_i , VO_2 defects and the 1048 cm^{-1} band upon isochronal annealing up to $\sim 500\text{ }^\circ\text{C}$.

The carbon substitutional (C_s) defect in Si

First we considered the single-carbon doped silicon, the relaxed structure of which is shown in Figure 3a. Table 1 lists the calculated bond distances and bond angles near the defect. Doping introduces a small distortion in the lattice with the formation of shorter Si–C bonds ($\sim 2.00\text{ \AA}$) than the Si–Si bonds calculated in bulk silicon (2.36 \AA) (refer to Table 1) and displacement of Si atom towards dopant. Furthermore, there is a slight perturbation in the Si–Si bond distances around the defect (refer to Table 1). The bond angles (Si–Si–Si) in a tetrahedral Si_4 unit in the Si

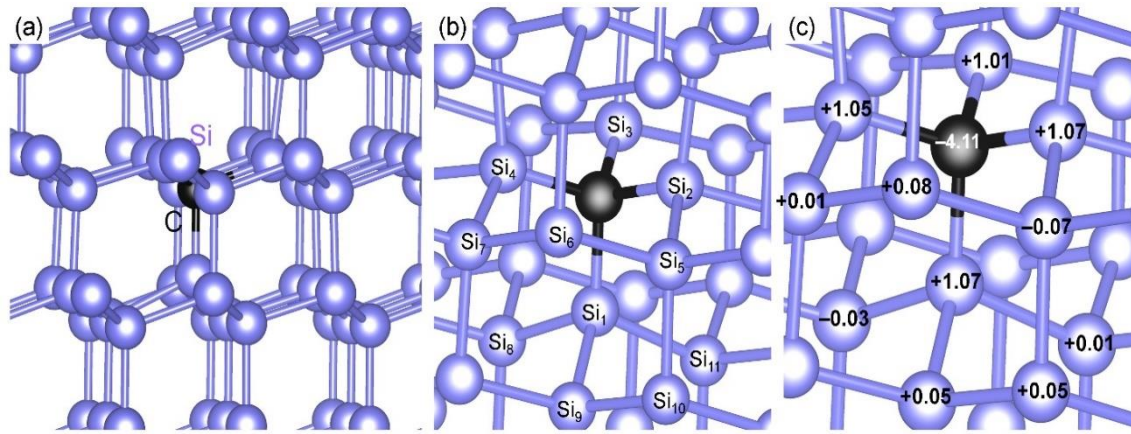


Fig. 3 (a) Relaxed structure of a single C-doped silicon, (b) a clear view of the defect structure and (c) Bader charges on the atoms near the defect.

Type of bond	Bond distance (Å)
Si ₁ -C	2.02
Si ₂ -C	2.02
Si ₃ -C	2.01
Si ₄ -C	2.01
Si ₁ -Si ₈	2.40
Si ₁ -Si ₉	2.40
Si ₁ -Si ₁₁	2.40
Si ₂ -Si ₅	2.41
Si ₅ -Si ₆	2.35
Si ₆ -Si ₇	2.35
Si ₄ -Si ₇	2.40
Si ₉ -Si ₁₀	2.35
Type of angle	Bond angle (°)
Si ₁ CSi ₂	109.53

Si ₁ CSi ₃	109.45
Si ₁ CSi ₄	109.40
Si ₂ CSi ₃	109.44
Si ₂ CSi ₄	109.47
Si ₈ Si ₁ Si ₉	102.54
Si ₈ Si ₁ Si ₁₁	102.72
Si ₉ Si ₁ Si ₁₁	102.66

Table I. Selected bond distances and bond angles in the relaxed structure of a single C-doped silicon.

are calculated to be 109.3°–109.6°. These values do not deviate much from those calculated in the CSi₃ tetrahedral unit. In the tetrahedral unit formed by the displaced Si atom (Si₁CSi₈Si₁₁), there is a slight elongation in the bond lengths (2.40 Å) and a significant reduction in the bond angles (102.5°) due to the upward movement of Si. Bader charge on the doped C is –4.11 showing the significant electron gain from the nearest neighbour Si atoms. This is further evidenced by the positive Bader charges (4×~1.00) on the four Si atoms attached to the C. This is clearly due to the higher electronegativity of C (2.55) than that of Si (1.90).⁴⁹

The C_sO_{2i} defect

Next we considered the oxygen di-interstitials in carbon-doped silicon (C_sO_{2i} defect). The optimised structure is shown in Figure 4, the density of states (DOS) and charge density plots are shown in Figure 5.

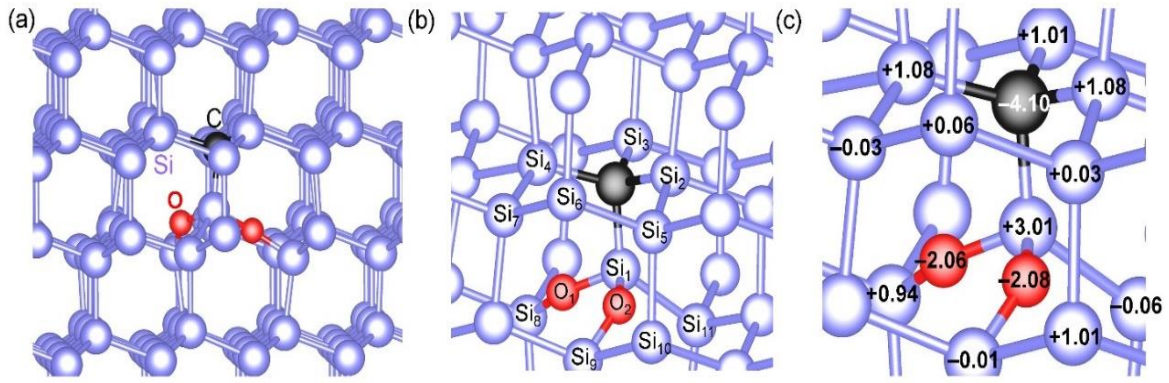


Fig. 4 The C_sO_{2i} defect. (a) Relaxed structure of oxygen di-interstitials at a single C-doped silicon, (b) a clear view of the defect structure and (c) Bader charges on the atoms near the defect.

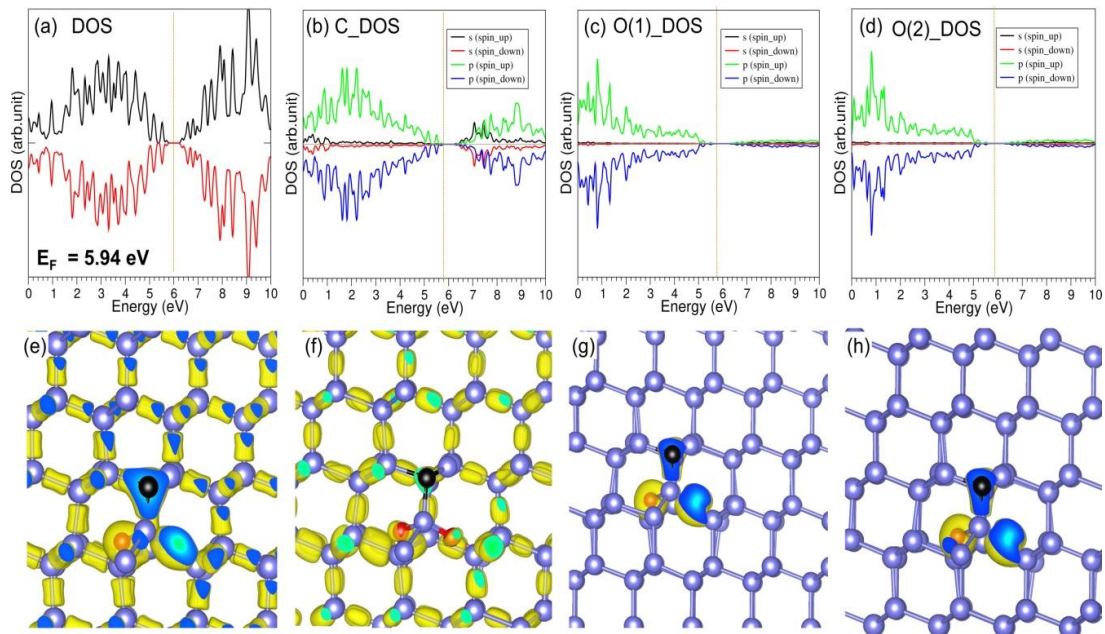


Fig. 5 (a) Total DOS plot, (b) atomic DOS plot of C, (c) atomic DOS plot of O_1 , (d) atomic DOS plot of O_2 , (e) total charge density plot; decomposed charge density plots associated with (f) C, (g) O_1 and O_2 . Charge density plots were constructed using an isosurface value of 0.06.

The selected bond distances and bond angles retrieved from the relaxed structure are shown in Fig. 6 in the LVM band estimation section (see below). Each oxygen atom

is bonded to two Si atoms in which one of them is directly bonded to C. The Si₃C tetrahedral unit exhibits shorter Si–C bond distances as discussed earlier. Interestingly, the Si₁–C bond distance is shorter by ~0.1 Å than that calculated in the tetrahedral unit of C-doped silicon. This is clearly due to the high Bader charge of +3.01 on the Si₁ which forms strong bond with C. The amount of electrons on the C (–4.10) is donated by four Si atoms (4×~1.00). The rest of the Bader charge of +2.00 on the Si₁ is due its donation of one electron each to the interstitial O atoms. The remaining one electron for each oxygen atom form O²⁻ is donated by adjacent Si atoms (Si₈ and Si₉). Though the donation of one electron is directly from Si₈ to O₁, the electron donation from Si₉ is not straight forward. That donation is obviously from the Si₁₀ but via Si₉ as Si₁₀–O₂ bond distance is too long (2.63 Å) for the direct donation. Both oxygen interstitials form bent structures with adjacent Si atoms with the bond angles of 141.68° and 150.92°.

The total DOS plot (see Figure 5a) shows that C–doped silicon is a semiconductor. The *p*-states of C are mainly located in the valence band showing the strong bonding nature of C with silicon bulk (see Figure 5b). This is further confirmed by the total charge density plot and decomposed charged density plot associated with C. Atomic DOS plots associated with interstitial oxygen show that *p*-states of oxygen atoms are strongly bound to silicon atoms they directly attached to and doped-C as evidenced by their decomposed charged density plots.

LVM band estimation of the C_sO_{2i} defect via the Dipole-Dipole Interaction Method

Fig. 6 demonstrates the lowest energy configuration of the C_sO_{2i} defect, in a unit cell, as derived from DFT calculations. The C_sO_{i(1)} and O_{i(2)} defects with reported apparent charges¹⁸ can be considered as two oscillating interacting dipoles. Mainly interested at frequencies around and above 1000 cm⁻¹, the investigation of the LVM lines of C_sO_{2i} was planned and carried out considering the perturbation of the oxygen related line⁷ of C_sO_{i(1)} at 1103 cm⁻¹ by the presence of a second oxygen interstitial atom (O_{i(2)}).

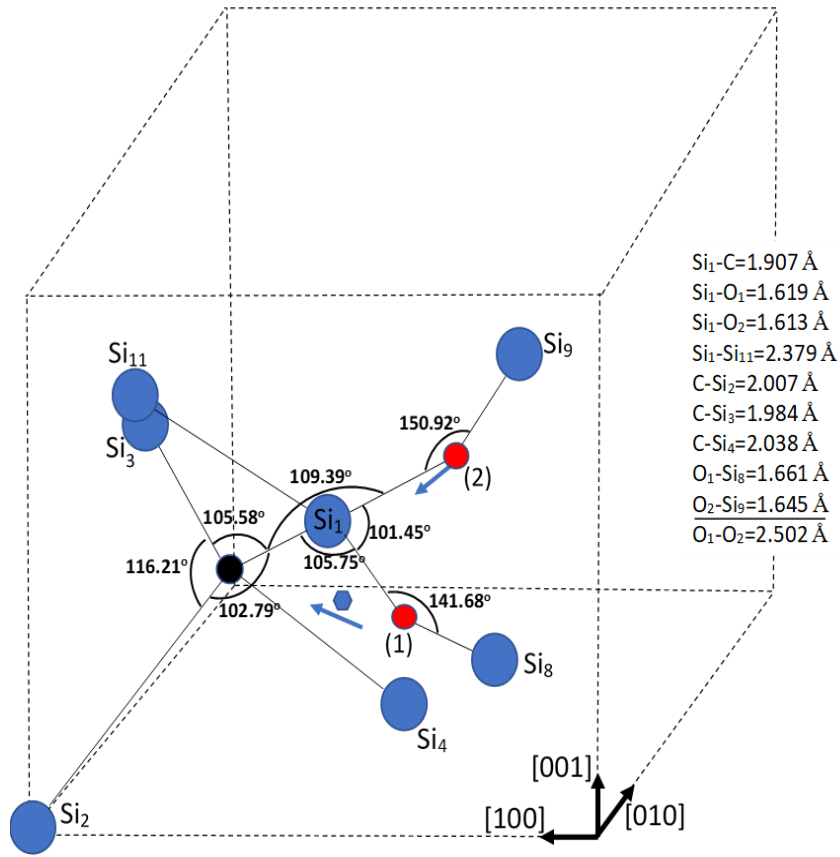


Fig. 6 Schematic representation of the C_sO_{2i} configuration in the unit cell. Blue, black and red circles correspond to Si, C and O atoms. Small blue hexagon is for the reduced mass, μ (see text). Si_1 , Si_3 , Si_4 atoms are located at the center of cubic sides and Si_8 , Si_{11} atoms are located respectively at $(1/4, -1/4, 1/4)$ and $(3/4, -1/4, 3/4)$ sites of the neighboring unit cell from paper plane to reader. Bond angles are noted on the figure and bond lengths are grouped in the inserted frame. Blue arrows indicate the oscillation directions of the $C_sO_{i(1)}$ and the $O_{i(2)}$ dipoles.

Regarding the $C_sO_{i(1)}$ dipole, C_s and $O_{i(1)}$ atoms are considered as one particle with mass equal to the reduced mass of oxygen and carbon atoms μ , located at the center of mass, at distance d from $O_{i(1)}$ atom. The reduced mass μ is derived from the relation

$$\mu = \frac{m_O m_C}{m_O + m_C} \quad (1)$$

while the distance d from the relation

$$d = \frac{m_C}{m_O + m_C} d_{C_s O_{i(1)}} \quad (2)$$

where $m_O=16$ amu, $m_C=12$ amu are the masses of the oxygen and carbon atoms, respectively and $d_{C_s O_{i(1)}} = 2.817 \text{ \AA}$ is the distance between the C_s and $O_{i(1)}$ atoms.

The calculated values for μ and d , are $\mu=11.38 \times 10^{-27}$ kg and $d = 1.206 \text{ \AA}$, respectively.

The effective charge of $C_s O_{i(1)}$ attributed to the 1103 cm^{-1} oxygen-related line is concentrated on the $C_s O_{i(1)}$ reduced mass μ , and is equal¹⁸ to $Z_{C_s O_{i(1)}} = 3.0 |e|$, where $|e|$ is the electron charge. The effective charge concentrated on the $O_{i(2)}$ atom is equal to¹⁸ $Z_{O_i} = 4.1 |e|$, where $|e|$ is the electron charge.

The procedure to evaluate the LVM frequencies of the $C_s O_{2i}$ defect utilizes a well-established^{50,51} method founded on the interaction of the $C_s O_{i(1)}$ and $O_{i(2)}$ dipoles. The force constant of the perturbed oscillating $C_s O_{i(1)}$ entity is $K_{C_s O_{i(1)}}$ and is given by the relation

$$K_{C_s O_{i(1)}} = \mu \left(\omega_{C_s O_{i(1)}} \right)^2 \quad (3)$$

where $\omega_{C_s O_{i(1)}}$ is the oxygen related LVM frequency of the $\omega_{C_s O_{i(1)}}$ defect at 1103 cm^{-1} . After substituting the values of μ and $\omega_{C_s O_{i(1)}}$ in Eq. (3) we find $K_{C_s O_{i(1)}} = 498.4 \text{ N/m}$.

We adopt the $C-\mu$ direction for the oscillation of the reduced mass of the $C_s O_{i(1)}$ dipole and the Si_1-Si_9 direction for the oscillation⁵² of the $O_{i(2)}$ dipole.

The formulae for the dipole moments $\mathbf{p}_{C_s O_{i(1)}}$ and $\mathbf{p}_{O_{i(2)}}$ become

$$\mathbf{p}_{C_s O_{i(1)}} = Z_{C_s O_{i(1)}} q_1 \hat{\mathbf{q}}_1, \quad \mathbf{p}_{O_{i(2)}} = Z_{O_{i(2)}} q_2 \hat{\mathbf{q}}_2 \quad (4)$$

where $\hat{\mathbf{q}}_1, \hat{\mathbf{q}}_2$ are the unit vectors along the oscillation directions of the dipoles. The potential energy of the interacting dipole moments is given by⁵³

$$U_{\text{int}} = \frac{\mathbf{p}_{C_s O_{i(1)}} \cdot \mathbf{p}_{O_{i(2)}} - 3(\hat{\mathbf{n}} \cdot \mathbf{p}_{C_s O_{i(1)}})(\hat{\mathbf{n}} \cdot \mathbf{p}_{O_{i(2)}})}{d_{\mu-O_{i(2)}}^3} \quad (5)$$

where $\hat{\mathbf{n}}$ is the unit vector along the direction that connects the two dipoles and $d_{\mu-O_{i(2)}} = 2.28 \text{ \AA}$ is the distance between them.

The motion of the two dipoles is described by the effective Hamiltonian

$$H = H_o + U_{\text{int}} = H_o + \lambda q_1 q_2 \quad (6)$$

where H_o corresponds to the kinetic and potential energy parts of the oscillation of the μ and $O_{i(2)}$ particles. By comparing Eq. (5) and (6) we derive the q -independent part λ , to be $\lambda=51.5 \text{ J/m}^2$.

The Hamiltonian of Eq. (6) has two normal modes with frequencies

$$\omega_{1,C_sO_{2i}} = \sqrt{\frac{K_{C_sO_{i(1)}} - \lambda}{\mu}} \quad (7)$$

and

$$\omega_{2,C_sO_{2i}} = \sqrt{\frac{K_{C_sO_{i(1)}} + \lambda}{\mu}} \quad (8)$$

For $K_{C_sO_{i(1)}} = 498.4 \text{ N/m}$ we find $\omega_{1,C_sO_{2i}}=1051.4 \text{ cm}^{-1}$ and $\omega_{2,C_sO_{2i}}=1166.3 \text{ cm}^{-1}$. The frequency at 1051.4 cm^{-1} , corresponding to the symmetric vibrational mode related to the 1103 cm^{-1} oxygen-related mode of the C_sO_i defect matches the detected line in our spectra at 1048 cm^{-1} , as well as the lines reported at earlier studies.^{25,32} The frequency at 1166.3 cm^{-1} , corresponding to the antisymmetric mode of the C_sO_{2i} related to the same oxygen-related LVM at 1103 cm^{-1} of the C_sO_i defect, also lies in the immediate vicinity of the experimentally detected line correlated with the C_sO_{2i} defect at 1094 cm^{-1} (deviation by $\sim 6.5 \%$).^{25,32} The above results enhance the assignment of the 1048 cm^{-1} to the C_sO_{2i} defect.

CONCLUSIONS

To summarize, the aim of the present study was to investigate the C_sO_{2i} defect in Si. Density functional theory (DFT) calculations were performed to find the most energetically favourable structures of oxygen di-interstitials near a carbon substitutional atom in silicon (C_sO_{2i}). The application of DFT technique allowed us to analyze the interaction of oxygen di-interstitials with carbon and to calculate the amount of charges on the atoms near the defects. Afterwards, the dipole-dipole interaction method was employed to calculate the Local Vibrational Mode (LVM) frequencies related with the most probable structure of the C_sO_{2i} defect, as suggested by DFT. Two bands at 1051.4 and 1166.3 cm^{-1} were estimated. These values are in agreement with the experimental values at 1048 and 1094 cm^{-1} ,

previously reported in the literature. Next, Infrared spectroscopy (IR) measurements carried out at Room Temperature (RT) detected a band at 1048 cm^{-1} raised in the spectra upon annealing out of the two bands of the vacancy-oxygen (VO) and the carbon interstitial-oxygen interstitial (C_iO_i) defects. The behavior of this band, its formation temperature and its thermal evolution strongly suggest correlation with the C_sO_{2i} defect. The other band of the structure at 1094 cm^{-1} was not detected in this study of RT measurements, probably because its weak signal is masked by the very strong band of oxygen interstitial (O_i) at 1106 cm^{-1} . This systematic study on the structure and properties of the C_sO_{2i} defect is expected to lead to further experimental and theoretical work on higher order carbon-oxygen defects that are important for Si based devices.

ACKNOWLEDGMENTS

T. Angeletos would like to thank A. S. Onassis Foundation for financial support for his Ph. D. thesis through scholarship (Grant No. G ZL 001-1/2015-2016).

DATA AVAILABILITY STATEMENT

The data that supports the findings of this study are available from the corresponding author upon reasonable request.

REFERENCES

- ¹A. Alkauskas, M. D. McCluskey, C.G. Van de Walle, J. Appl. Phys. **119**, 181101 (2016)
- ²M. Stavola, and W. Beall Fowler, J. Appl. Phys. **123**, 161561 (2018)
- ³H. M. Ayedh, E. V. Monakhov, and J. Coutinho, Phys. Rev. Mater. **4**, 064601 (2020).
- ⁴A. Chroneos, E. N. Sgourou, C. A. Londos, and U. Schwingenschlögl, Appl. Phys. Rev. **2**, 021306 (2015).
- ⁵D. Timerkaeva, D. Caliste, T. Deutsch, and P. Pochet, Phys. Rev. B **96**, 195306 (2017).
- ⁶P. Dong, X. G. Yu, L. Chen, X. Y. Ma, and D. R. Yang, J. Appl. Phys. **122**, 095704 (2017).

- ⁷G. Davies and R. C. Newman, in Handbook on Semiconductors, Materials Properties and Preparations, edited by T. S. Moss and S. Mahajan (North Holland, Amsterdam, 1994), p. 1557
- ⁸R. C. Newman and R. Jones, in Oxygen in Silicon, Semiconductors and Semimetals Vol 42, edited by F. Shimura (Academic press, Orlando, 1994) p. 289
- ⁹R. C. Newman, Infrared Studies of Crystal Defects (Taylor and Francis, London, 1973).
- ¹⁰B. Pajot and B. Clerjaud, Optical Absorption of Impurities and Defects in Semiconducting Crystals. II. Electronic Absorption of Deep Centres and Vibrational Spectra (Springer-Verlag, Berlin, 2013).
- ¹¹A. Borghesi, B. Pivac, A. Sassella, and A. Stella, J. Appl. Phys. **77**, 4169 (1995)
- ¹²H. Bender and J. Vanhellefont, in Handbook on Semiconductors Edited by S. Mahajan (Elsevier Science B.V., North Holland) Vol. 3b, 1637 (1994)
- ¹³W. Skorupa, R. A. Yankov, Mater. Chem. Phys. **44**, 101 (1996)
- ¹⁴C. A. Londos, M. S. Potsidi, and V. V. Emtsev, phys. stat. sol. (c) **2**, 1963 (2005)
- ¹⁵G. D. Watkins and J. W. Corbett, Phys. Rev. **121**, 1001 (1961)
- ¹⁶B. G. Svensson and J. L. Lindström, phys. stat. sol. (a) **95**, 537 (1987)
- ¹⁷C. A. Londos, phys. stat. sol. (a) **102**, 639 (1987), C. A. Londos, *ibid*, **92**, 609 (1985)
- ¹⁸S. P. Chappell, M. Claybourn, R. C. Newman and K. G. Barraclough, Semicond. Sci. Technol. **3**, 1047 (1988)
- ¹⁹G. Ferenczi, C. A. Londos, T. Pavelka, and M. Somogyi, J. Appl. Phys. **63**, 183 (1988)
- ²⁰D. Tsuchiya, K. Sueoka, and H. Yamamoto, Phys. Status Solidi A 1800615 (2019)
- ²¹S. D Brotherton and P. Bradley, J. Appl. Phys. **53**, 5720 (1982)
- ²²M. Siemienieć, F.-J. Niedernostheide, H.-J. Schlze, W. Sudkamp, U. Kellner-Werdehausen, and J. Lutz, J. Electroch. Soc. **153**, G108 (2006)
- ²³P. Pichler, in Intrinsic Point Defects, Impurities and their Diffusion in Silicon, edited by S. Selberherr (Springer Verlag, Wien, 2004).

- ²⁴R. C. Newman and R. S. Smith, *J. Phys. Chem. Solids*, **30**, 1493 (1969)
- ²⁵H. Yamada-Kaneta, Y. Shirakawa, C. Kaneta in *Early Stages of Oxygen Precipitation in Silicon*, edited by R. Jones (Kluwer Academic Publishers, Netherlands, 1996) pp. 389-396
- ²⁶Y. Shirakawa, H. Yamada-Kaneta, *J. Appl. Phys.* **80**, 4199 (1996)
- ²⁷C. Kaneta, T. Sasaki, H. Katayama-Yoshida, *Mater. Sci. Forum* **117-118**, 81 (1993)
- ²⁸C. A. Londos, E. N. Sgourou, A. Chroneos and V. V. Emtsev, *Semicond. Sci. Technol.* **26**, 105024 (2011)
- ²⁹N. Inoue, H. Ohyama, Y. Goto, and T. Sugiyama, *Physica B* **401-402**, 477 (2007)
- ³⁰C. A. Londos, A. Andrianakis, E. N. Sgourou, V. V. Emtsev and H. Ohyama, *J. Appl. Phys.* **109**, 033508 (2011)
- ³¹C. A. Londos, E. N. Sgourou, D. Timerkaeva, A. Chroneos, P. Pochet, and V. V. Emtsev, *J. Appl. Phys.* **114**, 113504 (2013)
- ³²L. I. Murin, and V. P. Markevich, J. L. Lindstrom, M. Kleverman, J. Hermansson, T. Hallberg, and B. G. Svensson, *Solid State Phenomena*, Vols **82-84**, 57 (2002)
- ³³L. I. Murin, V. A. Gurinovich, I. F. Medvedeva, and V. P. Markevich, *Inorganic Materials: Applied Research* **7**, 192 (2016)
- ³⁴P. Chen, X. Yu, X. Liu, X. Chen, Y. Wu, and D. Yang, *Appl. Phys. Lett.* **102**, 082107 (2013)
- ³⁵N. Inoue, T. Sugiyama, Y. Goto, K. Watanabe, H. Seki, and Y. Kawamura, *phys. stat. solidi C* **13**, 883 (2016)
- ³⁶G. Kresse and J. Furthmüller, *Phys. Rev. B* **54**, 11169 (1996).
- ³⁷G. Kresse and D. Joubert, *Phys. Rev. B* **59**, 1758-1775 (1999).
- ³⁸P. E. Blöchl, *Phys. Rev. B* **50**, 17953-17979 (1994).
- ³⁹J. P. Perdew, K. Burke and M. Ernzerhof, *Phys. Rev. Lett.* **77**, 3865-3868 (1996).
- ⁴⁰H. J. Monkhorst and J. D. Pack, *Phys. Rev. B* **13**, 5188-5192 (1976).

- ⁴¹W. H. Press, S. A. Teukolsky, W. T. Vetterling and B. P. Flannery, Numerical recipes in C (2nd ed.): the art of scientific computing (Cambridge University Press, 1992).
- ⁴²R. F. W. Bader, Theoretical Chemistry Accounts **105**, 276-283 (2001).
- ⁴³S. Grimme, J. Antony, S. Ehrlich and H. Krieg, J. Chem. Phys. **132**, 154104 (2010).
- ⁴⁴A. Chroneos, J. Appl. Phys. **105**, 056101 (2009)
- ⁴⁵A. Chroneos, C. Jiang, R. W. Grimes, U. Schwingenschlögl and H. Bracht, Appl. Phys. Lett. **95**, 112101 (2009).
- ⁴⁶A. Chroneos, H. Bracht, R. W. Grimes and B. P. Uberuaga, Mater. Sci. Eng. B, **154-155**, 72 (2008).
- ⁴⁷A. Chroneos, D. Skarlatos, C. Tsamis, A. Christofi, D. S. McPhail and R. Hung, Mater. Sci. Semicond. Proc. **9**, 640-643 (2006).
- ⁴⁸C. A. Londos, D. N. Aliprantis, G. Antonaras, M. S. Potsidi, and T. Angeletos, J. Appl. Phys. **123**, 145702 (2018)
- ⁴⁹D. R. Lide, CRC Handbook of Chemistry and Physics : A Ready-reference Book of Chemical and Physical Data /. 82nd ed. Boca Raton: CRC, 2004. Web.
- ⁵⁰N. V. Sarlis, C. A. Londos, L. G. Fytros J. Appl. Phys. **81**, 1645 (1997)
- ⁵¹M. S. Potsidi and C. A. Londos J. Appl. Phys. **100**, 033523 (2006)
- ⁵²M. D. Mc Cluskey, J. Appl. Phys. **87**, 3593 (2000)
- ⁵³J. Jackson, in *Classical Electrodynamics* (Wiley, New York, 1975), p. 136

Declaration of interests

The authors declare that they have no known competing financial interests or personal relationships that could have appeared to influence the work reported in this paper.

The authors declare the following financial interests/personal relationships which may be considered as potential competing interests: